ELSEVIER

Polymer 40 (1999) 3753–3761

polymer

Shrinkage behaviour of uniaxially drawn poly(ethylene 2,6-naphthalate) films

G. Schoukens*, M. Verschuere

University of Ghent, Faculty of Applied Sciences, Department of Applied Mechanics, Sint-Pietersnieuwstraat 41, B-9000 Ghent, Belgium

Received 2 July 1998; accepted 4 August 1998

Abstract

Amorphous films of poly(ethylene 2,6-naphthalate) (PEN) were drawn isothermally at 145°C up to the desired draw ratios mainly to study structure formation during uniaxial drawing by differential scanning calorimetry and to characterise the shrinkage behaviour of the drawn films with or without heat treatment. During drawing, a rigid phase structure is induced and the amount of induced rigid phase structure is linearly related to the square root of the extra first strain invariant. The stress–strain curves are characterised by a necking behaviour and the end of the yielding or necking is reached when the amount of induced rigid phase is attaining 50%. The stretching behaviour of PEN is characterised more by the strain induced rigid phase formation (SIRP) than by the stress or strain induced crystallisation. The shrinkage behaviour is characterised by two regimes. A first one for draw ratios below the necking behaviour where the films shrink back to their original length for temperatures between 100 and 140°C with a mid-value of 120°C, corresponding to the glass transition temperature of the amorphous phase. The second regime, for draw ratios above the necking behaviour is characterised by a shrinkage behaviour for temperatures between 120 and 160°C, with a mid-value of 140°C, corresponding to the transition temperature of the induced rigid phase structure. In this regime, the films never shrink back below the draw ratio after necking and a linear relation between the initial draw ratio and the final draw ratio after shrinkage is obtained. A heat treatment of the oriented films with fixed ends stabilises the induced structures and the shrinkage of these heat-set films is zero for temperatures up to the heat-setting temperature.

Keywords: Poly(ethylene naphthalate); Stress–strain curve; DSC

1. Introduction

Poly(ethylene 2,6-naphthalate) (PEN) is a polyester whose preparation was first reported as long ago as 1948 [1]. PEN is produced by condensation polymerisation of 2,6-naphtalenedicarboxylic acid and ethylene glycol [2–4]. There has, however, been increasing interest in its commercial use since recent indications [5,6] that the dicarboxylic acid monomer becomes available in large-scale quantities. PEN molecules contain naphthalene rings, which are stiffer than those of poly(ethylene terephthalate) (PET). The important aspect of PEN is the influence of an increased chain stiffness on the mechanical and thermal properties of the polymer. This polymer, like PET, can be formed into amorphous form by quenching from the melt or it can be crystallised either by slow cooling from the melt or by stretching between the glass transition temperature and the cold crystallisation temperature. PEN exhibits a glass transition temperature of about 120°C, which makes it quite attractive as a high-temperature polymer for film, tape and moulding applications. PEN possess oxygen barrier properties four to five times higher than those of PET and makes PEN attractive for packaging applications.

One of the unusual characteristics of PEN is that it shows necking behaviour upon stretching from the amorphous state above the glass transition temperature [7,8]. Some authors reported that this neck formation is a result of a highly co-operative orientation of the naphthalene planes parallel to the surface of the film. This behaviour resembles an isotropic to nematic structural transition which occurs in highly localised regions of the sample.

It has been reported that PEN also has two crystal forms (α and β) and both are triclinic depending on the crystallisation temperature [9]. Crystallising at 180°C yields the α form as reported by Mencik [2] while crystallising at 240°C yields the β form. Recent X-ray work [10] has suggested the presence of a mesophase in addition to the crystal form. In this mesophase structure, the molecular chains are in registry with each other in the meridional direction but not fully crystallised in the equatorial direction. The emergence of this structure is due to drawing of PEN at temperatures of

---

* Corresponding author. Tel.: + 32-9-264-32-49; Fax: + 32-9-223-73-26; e-mail: gustaaf.schoukens@rug.ac.be

PII: S0032-3861(98)00598-9

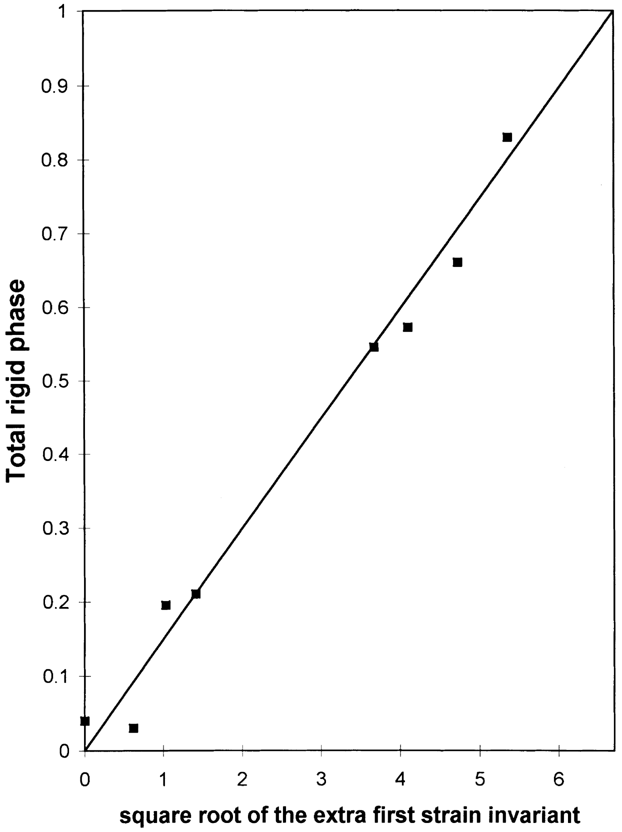

Fig. 1. Total rigid phase as obtained from DSC measurements in relation to the first strain invariant I_{1e}.

120 or 150°C [11]. This structure persisted upon annealing at 180°C or 200°C which leads to the conclusion that this mesophase structure is stable at high temperature.

In the first article [12], we represented the amount of rigid phase structure f_r as a function of I_{1e}, the extra first strain invariant and equal to $I_1 - 3$, and a correlation between these two was experimentally obtained, so that the fraction f_r varied between 0 and 1 with the square root of I_{1e}. This relationship was expressed by the following equation:

$$f_r = I_{1e}^{0.5}/I_{1e,\max}^{0.5}$$

The value of $I_{1e,\max}$ corresponds to the maximum attainable draw ratio, equal to 6.9 at 145°C, and is reproduced in Fig. 1.

In the same article, we compared the stress–strain curve with f_r during drawing. We observed that when f_r reached 50%, for a draw ratio of 4, a dramatic increase of stress was measured, as reproduced in Fig. 2. Actually, the dramatic increase in stress suggests a critical degree of rigid phase structure, similar to a percolation threshold accompanied by an inversion of the continuous phase, above which the rigid phase structure is drawn. When f_r is less than 50% the amorphous phase is the continuous phase, with the rigid phase dispersed therein. If f_r is greater than 50%, phase inversion takes place and the rigid phase is forming the continuous phase with an amorphous phase dispersed therein.

The shrinkage behaviour of PET is rather complicated, but well documented, and an increased dimensional stability of biaxially oriented PET containers and films can be obtained by heat setting [13]. Even with heat setting, the hot fill temperature of PET containers is reported to be limited to 85–95°C [14,15], and for certain applications,

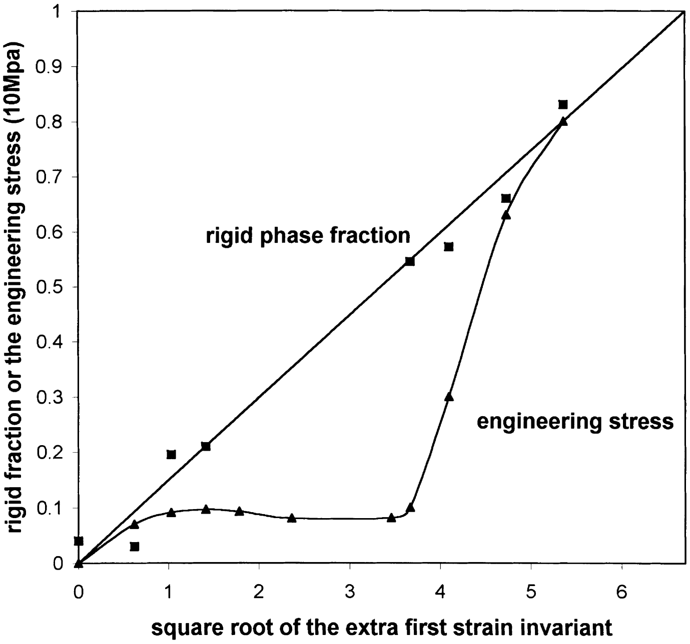

Fig. 2. Comparison between the amount of induced rigid phase as obtained from DSC measurements and the measured engineering stress as a function of the draw ratios at 145°C. Here, engineering stress = load/initial cross-sectional area.

Table 1
The uniaxially drawn PEN samples

Sample	Drawing ratio (λ)	Drawing temperature (°C)	Drawing speed (mm/min)
PEN0	1	–	–
PEN1	1.4	145	50
PEN2	1.7	145	50
PEN3	2	145	50
PEN4	4	145	50
PEN5	4.3	145	50
PEN6	5	145	50
PEN7	5.6	145	50

for example hot fill applications, shrinkage properties are inadequate.

In this article we present our results on the shrinkage behaviour of oriented PEN films as influenced by uniaxial drawing at different draw ratios and heat treatment at different temperatures by using differential scanning calorimetry (DSC) measurements in addition to the shrinkage curves to perform a structural analysis.

2. Experimental

2.1. Materials

Poly(ethylene 2,6-naphthalene) (PEN) with an intrinsic viscosity of 0.65 dl/g used in this study was provided in film form and in pellet form by ICI plc. The thickness of the film was 0.65 mm.

2.2. Thermal analysis

The thermal properties of unoriented and oriented PEN-films were determined using Universal V1.6I TA Instruments at a heating rate of 10°C/min in a dry nitrogen atmosphere. The glass transition temperature (T_g) for unoriented PEN sample was observed to be around 112°C, the cold crystallisation peak temperature around 197°C and the melting temperature at 271°C. The heat of cold crystallisation is around 35 J/g, the heat of fusion equals 38.64 J/g with a heat capacity increase at T_g of 0.3360 J/(g K) or 84 J/(K mol).

2.3. Crystallinity

The crystallinity of the films before and after orientation was determined using DSC thermograms. The crystallisation exothermic enthalpy, $\Delta H_{\text{cold crystallisation}}$ or ΔH_c, was substracted from that of the melting endotherm, $\Delta H_{\text{melting}}$ or ΔH_m, to determine the amount of apparent crystallinity initially present in the samples. Crystallinity of the films was calculated according to:

$$\text{Crystallinity (\%)} = \Delta H_{\text{exp}} \times 100/\Delta H_f$$

where $\Delta H_{\text{exp}} = \Delta H_m - \Delta H_c$ and ΔH_f is the heat of fusion for 100% crystalline PEN, 103.4 J/g [16].

2.4. Stress–strain behaviour

To determine the uniaxial stress–strain behaviour, an Instron tensile tester (Model 4202) equipped with a high-temperature chamber was used. A dumbbell-shaped test strip (total length 30 mm), with a narrow mid-section of 5 mm width and 12.5 mm length, was stretched at a drawing rate of 50 mm/min. Before drawing, the sample was equilibrated at the desired temperature for 10 min in a preheated convection oven and drawn to selected draw ratios at selected rates.

The amorphous PEN films were drawn uniaxially at 145°C, at a drawing speed of 50 mm/min; the drawing ratios are listed in Table 1. The draw ratio λ is the ratio of the extended length to the original length determined from displacement of ink marks on the narrow mid-section of the dumbbell-shaped test strip.

2.5. Crystallinity and rigid amorphous phase

PEN provides a new example of a polymer that may possess in the oriented state a crystalline and a rigid amorphous fraction [16,17], which may be a nematic and/or mesophase structure. The rigid amorphous fraction does not contribute to the increase in the heat capacity at T_g and devitrifies only at temperatures [16] (430 K) well above T_g. Similar behaviour was found in several high-melting temperature polymers with phenylene groups in the main chain. The overall rigid fraction f_r, comprising the rigid amorphous phase and the crystalline phase, is computed from the heat capacity C_p by setting

$$f_r = 1 - [\Delta C_p(m)/\Delta C_p(a)]$$

where $\Delta C_p(m)$ and $\Delta C_p(a)$ represent the measured and total amorphous heat capacity increase at T_g, respectively. The amount of crystallinity, in turn, is determined by DSC:

$$w^c = \Delta H_{\text{exp}}/\Delta H_f$$

where ΔH_{exp} and ΔH_f are the measured and 100% crystalline heat of fusion, respectively.

In the non-oriented state, where the two phase model of amorphous and crystalline phase is valid, the fraction f_r is equal to w^c. If f_r is greater than w^c, a rigid amorphous phase exists about T_g which can be quantified.

All the samples were measured with an updated computer-interfaced Universal V1.6I TA Instruments. The heat capacity measurements were performed in the temperature range 20–300°C. The DSC was calibrated using the standard procedures.

The DSC melting traces for the uniaxially drawn samples PEN1–7 showed that the lowest temperature of the glass transition zone, T_{gl} and the melting temperature T_m are almost independent of the draw ratio.

By representing the amount of rigid phase structure f_r as a function of I_{1e}, the extra first strain invariant and equal to $I_1 - 3$, a correlation between the two was experimentally

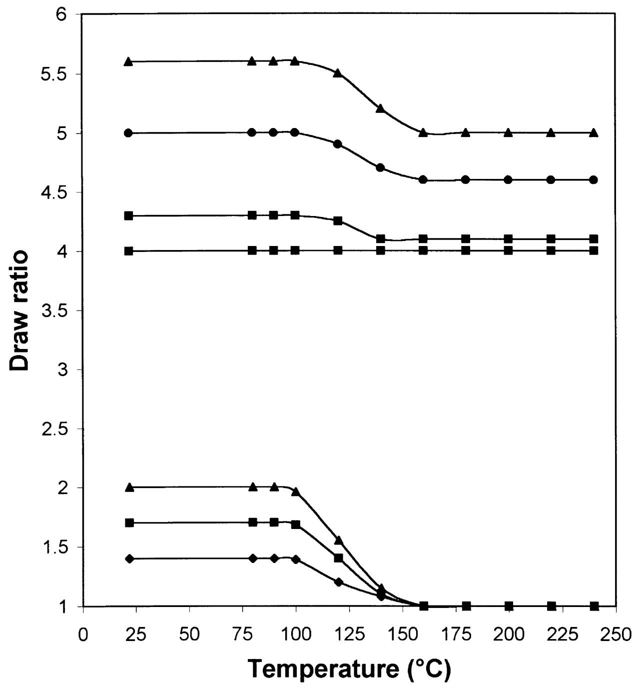

Fig. 3. Variation of the draw ratio after shrinkage with free ends as a function of temperature.

obtained [12]. The fraction f_r varied between 0 and 1 with the square root of I_{1e} and this relationship can be expressed by the following equation, for samples uniaxially stretched at 145°C and cooled quickly to room temperature:

$$f_r = I_{1e}^{0.5}/6.7$$

The value of 6.7 corresponds to the maximum attainable draw ratio at 145°C (6.9).

2.6. Heat setting

Samples cut from the uniaxially stretched films were mounted with fixed ends in a steel frame. The mounted samples were then placed in a circulating air oven for 15 min at the desired temperature (170 and 220°C). After 15 min, the frame with the fixed samples was removed from the circulating air oven and allowed to cool to room temperature before the samples were removed from the frame. Previous studies have shown that a treatment time of 15 min is sufficient to attain the desired temperature in the circulating air oven and to obtain a constant density value of the heat setted films.

2.7. Shrinkage

The oriented samples, without or with heat setting, were placed unconstrained in a circulating air oven at the selected temperature. After 30 min, the samples were removed, allowed to cool to room temperature and the displacement of ink marks on the samples was measured and controlled by the thickness variation of the samples. The influence of the shrinkage behaviour is expressed by the measured draw ratio λ and is equal to the ratio of the extended length between the ink marks after stretching and shrinkage on the original length.

3. Results and discussion

Shrinkage at temperatures between 80 and 260°C was measured. The results of the shrinkage measurements at the selected temperatures for the drawn samples PEN1–7 as indicated in Table 1 are represented in Fig. 3.

At temperatures up to 100°C the drawn samples showed

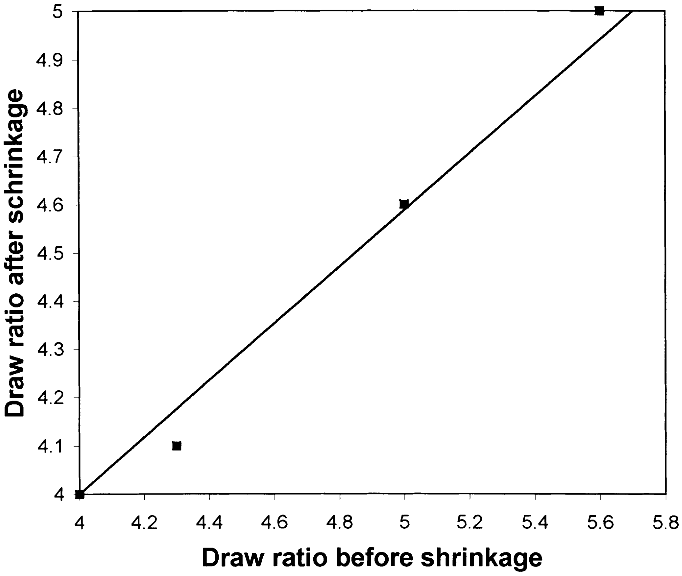

Fig. 4. The final draw ratio after shrinkage versus the initial draw ratio.

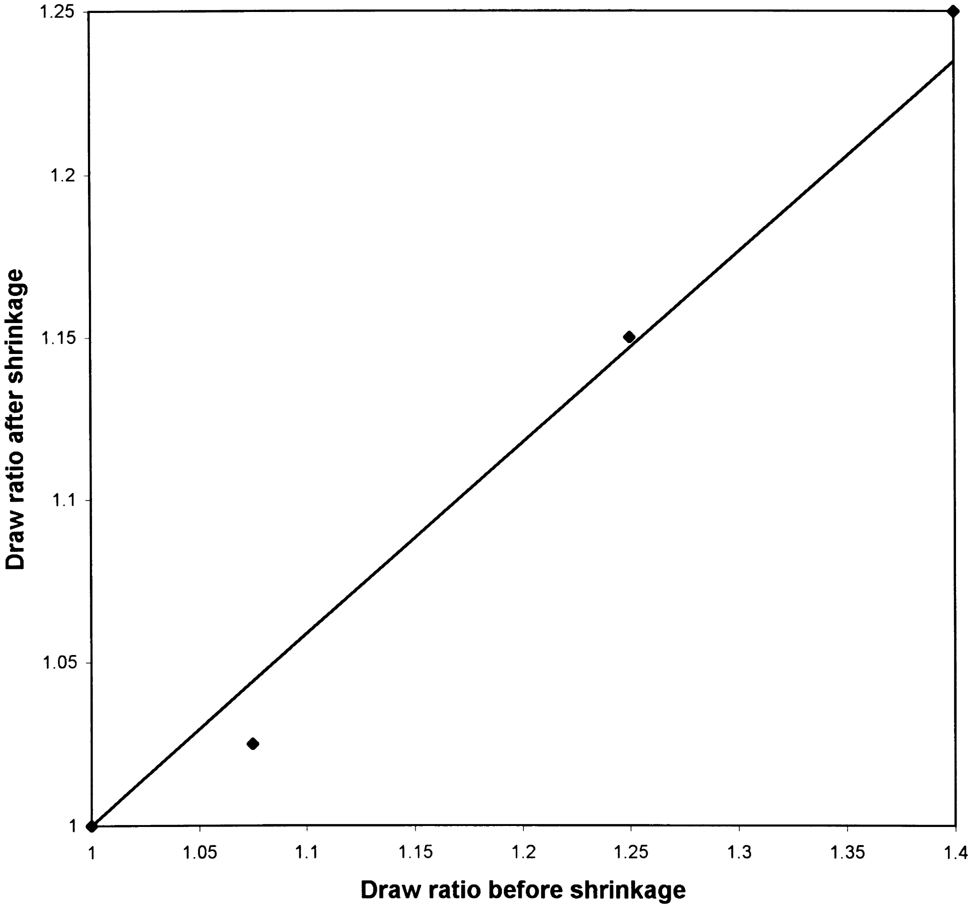

Fig. 5. Recalculated draw ratio after maximum shrinkage versus the recalculated initial draw ratio.

no measurable shrinkage. For the drawn samples PEN1–3 with a draw ratio below the necking behaviour ($\lambda < 2.2$), shrinkage increased with temperature above 100°C and with increasing degree of stretching up to 140°C. The samples shrank to their original length at temperatures above 140°C. The mid-value temperature of the shrinkage behaviour is situated around 120°C, corresponding to the glass transition temperature of the amorphous phase.

For the samples PEN4–7, drawn with necking, the measured shrinkage behaviour was totally different. For the drawn sample with a draw ratio of 4, just after necking, shrinkage was practically zero for temperatures up to 240°C. This is a remarkable result. No shrinkage was measured for the drawn sample at the end of the necking zone, accompanied by a phase inversion from the amorphous phase to the rigid amorphous phase as continuous phase. This can be explained by the facts that the rigid amorphous phase is stable up to 240°C and is not in a stretched state at the moment of phase inversion.

For samples further drawn after the necking behaviour, PEN5–7, shrinkage started at 120°C and increased up to 160°C, with a mid-value of 140°C. This corresponds to a transition temperature of the rigid amorphous phase of 150°C as deduced from the stress–strain curves and the DSC measurements. These samples showed a certain degree of shrinkage, with a constant value for temperatures above 170°C, but never shrank below the draw ratio of necking. If we plot the final draw ratio after shrinkage for temperatures above 170°C versus the initial draw ratio, a linear relationship can be deduced between these two parameters as demonstrated in Fig. 4.

If we take sample PEN4, with a draw ratio of 4 corresponding to the draw ratio of the necking behaviour, as the starting sample for drawing and recalculate the draw ratios of samples PEN5–7 taking that sample as reference sample, an interesting result is obtained as represented in Fig. 5.

The linear relationship between the calculated draw ratios after shrinkage for temperatures above 170°C and the initial draw ratio, related to sample PEN4, is also observed and the final draw ratio after shrinkage is 60% of the initial draw draw ratio with a corresponding constant shrinkage value of 40%. In this case, the rigid amorphous phase is elongated after phase inversion and 40% of the induced supplemental elongation is recovered during shrinkage at high temperatures.

The uniaxially drawn samples, heatset with fixed ends at 220°C for 15 min, showed no measurable shrinkage at temperatures up to 200°C. A small shrinkage value is

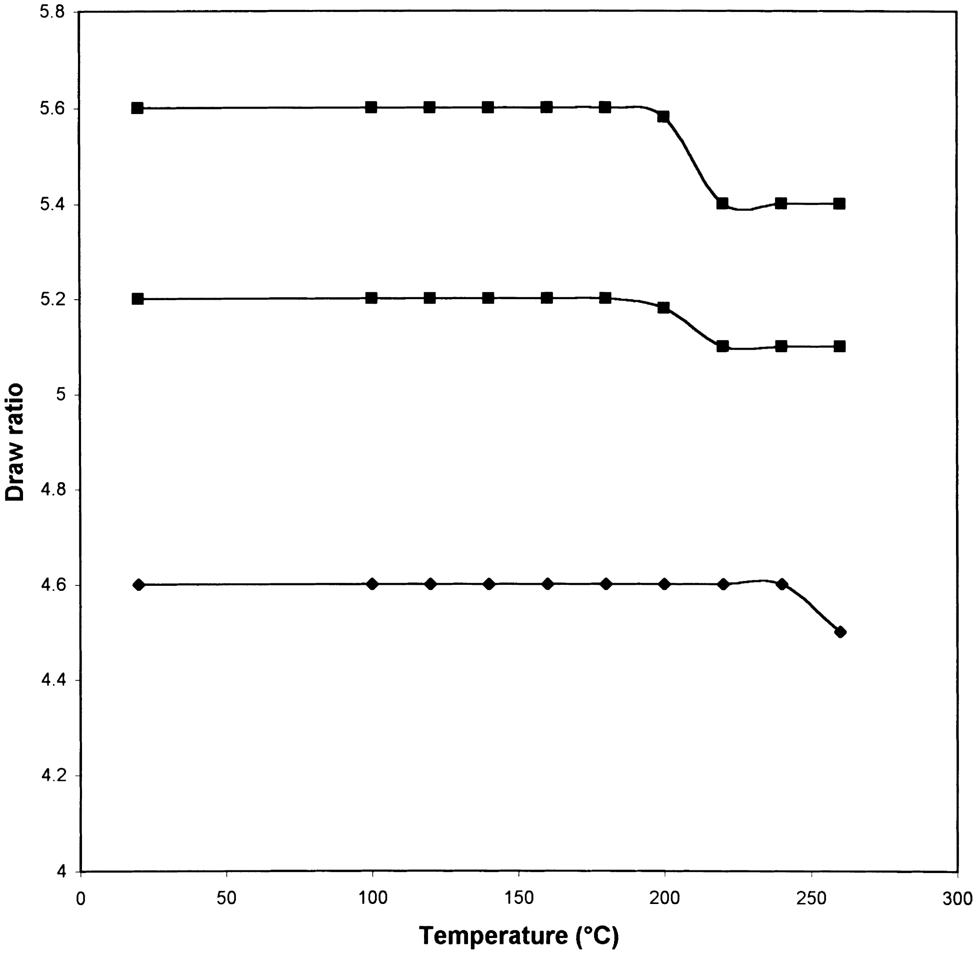

Fig. 6. Shrinkage of heatset drawn samples with fixed ends at 220°C as a function of temperature.

obtained for temperatures between 220 and 260°C as represented in Fig. 6.

The uniaxially drawn samples, heatset with fixed ends at 170°C for 15 min, showed no measurable shrinkage at temperatures up to 160°C. For temperatures higher than 160°C, a shrinkage is measured that increases linearly with temperature up to 260°C as represented in Fig. 7.

The heatsetting with fixed ends stabilises the oriented structure up to temperatures approaching the heatsetting temperature and may be explained by the mobility of the induced rigid phase structure during drawing at temperatures higher than 160°C, 10°C higher than the transition temperature of the rigid phase structure as obtained from the stress–strain curves. A reorganization of the induced structure during drawing can take place, accompanied by relaxation of the induced stresses, due to the mobility of the rigid phase structure at those elevated temperatures and before further crystallisation takes place.

The shrinkage behaviour of uniaxially drawn PEN is different in many respects from that of PET and the effect of heatsetting with fixed ends on the shrinkage behaviour is also different in many aspects from that observed for oriented PET samples.

The DSC melting traces of samples PEN4–7, after shrinkage with free ends at 240°C, are quite different from those measured before shrinkage and the measured curve of PEN4 is reproduced in Fig. 8.

The DSC melting traces for the other samples are comparable. The transition zone becomes larger, extending from 112°C to 149°C, with a T_g of 130°C with an accompanying ΔC_p value of 0.2711 J/g °C, compared with a glass transition zone of 109–119.7°C, T_g of 114°C and ΔC_p value of 0.1490 J/g °C before shrinkage. A second difference with the DSC melting traces measured before shrinkage is the presence of a small melting peak ocurring about 10°C above the heatset temperature with a heat of fusion of 8.04 J/g. The second melting peak, the largest one, is observed at 265.7°C with a heat of fusion of 45.74 J/g. The two melting peaks are the same for the other samples PEN5–7. The total heat of fusion corresponds to 54% crystallinity in the samples. An endothermic low melting peak appears in the DSC thermograms of the oriented samples after shrinkage with free ends. During annealing and shrinkage small crystallites are produced with a low degree of perfection and a corresponding low melting temperature. The high melting peak temperature remains almost constant with a constant value

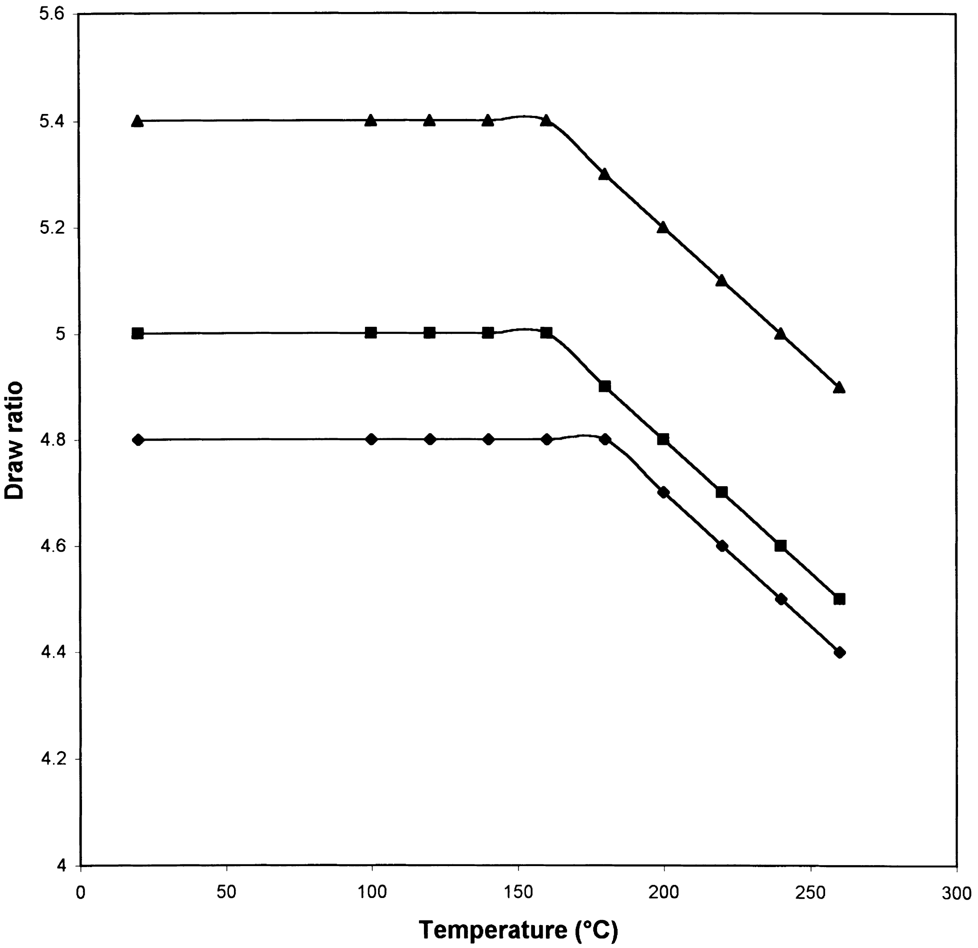

Fig. 7. Shrinkage for drawn samples heatset with fixed ends at 170°C as a function of temperature.

of the heat of fusion. The melting temperature of the low melting peak is influenced by the selected temperature of shrinkage and varies linearly with the shrinkage temperature from 228.4°C for a shrinkage temperature of 220°C to 249.5°C for a shrinkage temperature of 240°C. The heat of fusion of the low melting temperature increased from 3.1 J/g for a shrinkage temperature of 220°C to 8.04 J/g for a shrinkage temperature of 240°C. The low melting temperature may be influenced by the degree of crystal perfection as well as by the induced crystalline structure as folded lamellar, fibrillar or fringed micelle crystalline structure. The measured values of the heat capacity change in the glass transition zone is higher for the samples after shrinkage than for the oriented sample without heat treatment. Extrapolation of the measured values of ΔC_p to a zero value of the extra first strain invariant I_{1e} gives a value of 0.6 J/g instead of 0.34 J/g before the shrinkage measurements. Clearly, there must be an influence of the oriented and stabilised structure on the thermal behaviour of the amorphous phase. The heat capacity change in the transition zone, together with the draw ratio after shrinkage and the related fraction of amorphous phase calculated from the relation between the content of amorphous hase and draw ratio, as represented in Fig. 1, the degree of crystallinity calculated from the DSC measurements and the calculated fraction of rigid amorphous phase are presented in Table 2.

These calculated values of the different fractions present in the oriented sample after shrinkage with free ends at 240°C indicate that a portion of the rigid amorphous phase, induced during drawing, is transformed into a crystalline structure. For the oriented sample with draw ratio of 4, just outside the necking behaviour, the rigid amorphous phase is practically totally transformed into a crystalline structure. The uniaxially drawn samples with an initial draw ratio higher than 4 still contain a certain fraction of rigid amorphous phase after shrinkage at 240°C and the amount is also here a function of the square root of the first extra strain invariant I_{1e}, calculated with the draw ratio measured after shrinkage with free ends.

4. Conclusions

The drawing behaviour of amorphous PEN is characterised by a necking behaviour and the end of yielding or necking is reached when the amount of the induced rigid

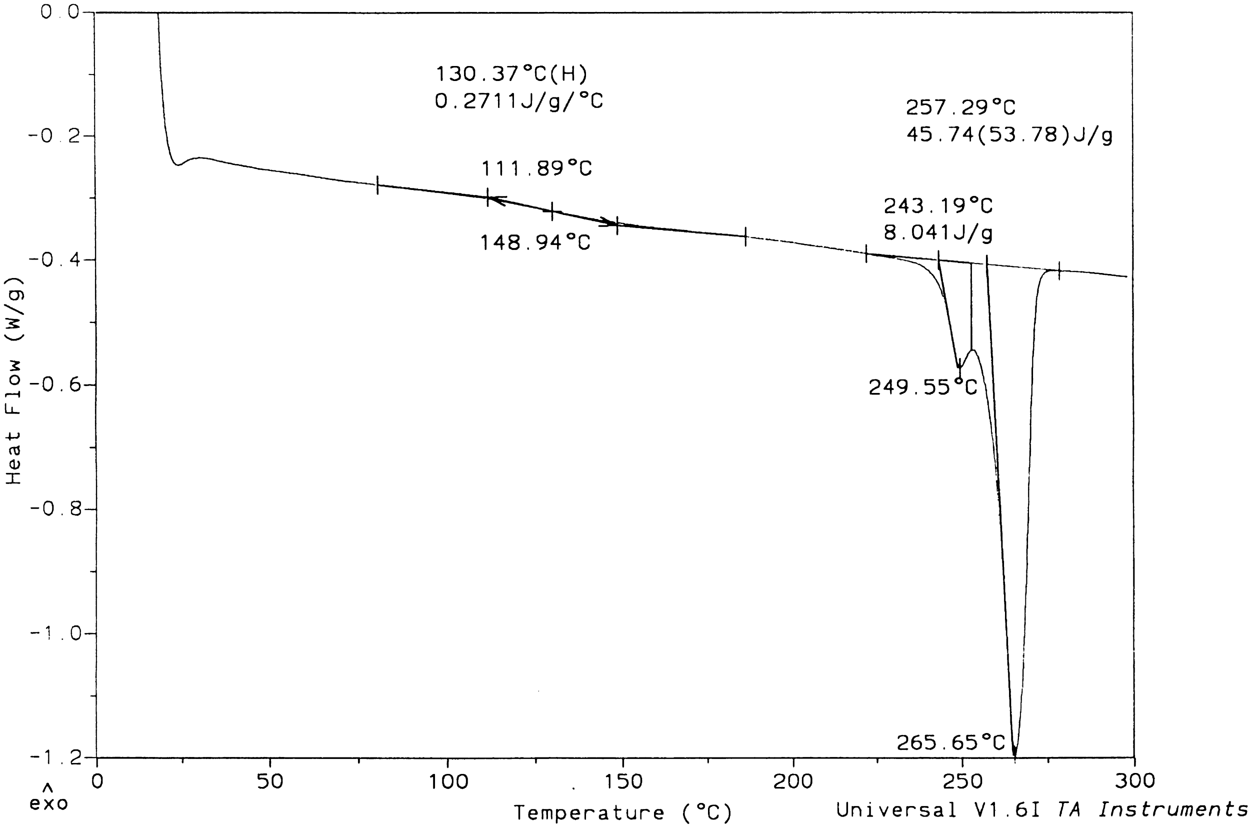

Fig. 8. DSC melting trace of PEN4 after shrinkage with free ends at 240°C.

phase attains 50%. The stretching behaviour of PEN is characterised more by the SIRP than by the stress or strain induced crystallisation.

The shrinkage behaviour is characterised by two regimes. One is for draw ratios below the necking behaviour where the films shrink to their original length, comparable with the shrinkage behaviour of PET at small draw ratios. The second regime, for draw ratios above the necking behaviour is characterised by a shrinkage behaviour that is different in many aspects from the shrinkage behaviour of PET. The uniaxially drawn samples are characterised by a small value of shrinkage for temperatures between 120 and 160°C and no further shrinkage for higher temperatures. The films never shrink back below the draw ratio corresponding with necking and a linear relationship is obtained between the initial draw ratio and the final draw ratio after shrinkage at temperatures above 160°C. From DSC measurements, a structure change is observed whereby a part of the induced rigid phase is transformed into a crystalline structure and the sample drawn at a draw ratio corresponding to the necking behaviour, with no shrinkage even with free ends, ondergoes a quasi complete transformation of the rigid amorphous phase into a crystalline phase.

Heat treatment of the oriented films with fixed ends stabilises the induced structures and the shrinkage of these heatset films is zero for temperatures approaching the

Table 2
The different structure fractions calculated after uniaxially drawing of PEN followed by free shrinkage at 240°C. Here, f_a is the fraction of amorphous phase, f_{cr} is the fraction of crystalline phase and f_{riga} is the fraction of rigid amorphous phase

Draw ratio after shrinkage	Square root of the first extra strain invariant	f_a	f_{cr}	f_{riga} after shrinkage	f_{riga} before shrinkage
4	3.67	0.43	0.54	0.03	0.14
4.1	3.78	0.42	0.54	0.04	0.14
4.6	4.31	0.34	0.54	0.12	0.17
5	4.73	0.28	0.54	0.18	0.33

heatsetting temperature. Heatsetting of the oriented PEN films can completely eliminate shrinkage for temperatures up to the heatsetting temperature.

Acknowledgements

The authors are deeply grateful to ICI plc who kindly supplied us with the amorphous PEN films and to Prof. E. Schacht (University of Ghent, Faculty of Sciences) for provision of DSC measurement facilities.

References

[1] Cook JG, Huggill HPW, Lowe AR. Br. Patent GB604073, 1946.
[2] Mencik Z. Chem Prim 1967;17:78.
[3] Cakmak M, Wang YD, Simhambhatla M. Polym Eng Sci 1990;30(2):721.
[4] Desai AB, Wilkes GL. J Pol Sci Symp 1974;46:291.
[5] Chem Week, 7 (6 March 1991).
[6] Chem Marketing Reporter (12 July 1993).
[7] Cakmak M, Lee SW. Polymer 1995;36:4039.
[8] Murakami S, Yamakawa M, Tsuji M, Kohjiya S. Polymer 1996;37:3945.
[9] Buchner S, Wiswe D, Zachmann HG. Polymer 1989;30:480.
[10] Jakeways R, Klien JL, Ward IM. Polymer 1996;37:3761.
[11] Saw CK, Menczel J, Choe EW, Hughes UR. SPE Antec Tech Pap 1997;II:1610.
[12] Schoukens G. Polymer (in press).
[13] Jabarin SA. SPE 11th Annual High Performance Blow Molding Conference, Cleveland, October 17–18, 1995. Society of Plastics Engineers, Cleveland Section.
[14] Maruhashi Y, Asada T. Polym Eng Sci 1992;32:481.
[15] Maruhashi Y, Asada T. Polym Eng Sci 1996;36:483.
[16] Cheng SZD, Wunderlich B. Macromolecules 1988;21:789.
[17] Cheng SZD, Janimak JJ, Zhang A, Guan J, Chu AL. Polym Bull (Berlin) 1988;20:449.